Quantifying SST errors from an OGCM in relation to atmospheric forcing variables

A. Birol Kara [a],[*],[1], Alan J. Wallcraft [a], Harley E. Hurlburt [a], Wei-Yin Loh [b]

[a] Oceanography Division, Naval Research Laboratory, Stennis Space Center, MS, USA
[b] Department of Statistics, University of Wisconsin, Madison, WI, USA

ARTICLE INFO

ABSTRACT

The relationship between various atmospheric variables at the sea surface and climatological monthly means of sea surface temperature (SST) is investigated over the global ocean. The goal is to quantify the change in SST that results solely from variations in a particular atmospheric variable. This is accomplished using a series of numerical simulations from an atmospherically-forced ocean general circulation model (OGCM). It is first demonstrated that SST variations at all latitudes are generally strongly and positively correlated with increases in near-surface air temperature, and vapor mixing ratio and net shortwave radiation at the sea surface, while they are often moderately and negatively correlated with increases in near-surface wind speed. There is only a weak and negative relationship between variations in SST and those in net longwave radiation at the sea surface. Variations in the net shortwave radiation and vapor mixing ratio are found to have more influence in driving the seasonal cycle of SST than other atmospheric variables. Global averages of slope values from the least squares fit indicate that a 1 °C change in air temperature results in $\approx$0.2 °C change in SST. Similarly, a 1 g kg^{-1} change in vapor mixing ratio gives $\approx$0.4 °C change in SST, and 10 W m^{-2} change in shortwave (longwave) radiation results in $\approx$0.13 °C ($\approx$0.07 °C) change in SST. All these values vary regionally, and are neither constant nor in the same direction everywhere. In addition, some atmospheric variables are already correlated to each other. Therefore, a fractional factorial design which involves the joint effects of all atmospheric variables on SST at the same time is further applied. Results from the factorial design are somewhat consistent with the simple linear regression analysis, in that a 2 °C increase in air temperature can typically give an increase in SST, generally ranging between 0.5 and 0.8 °C over the global ocean.

Published by Elsevier Ltd.

1. Introduction and motivation

Spatial and temporal variability of sea surface temperature (SST) is closely related to the substantial heat content of the ocean mixed layer, which itself is largely influenced by atmospheric conditions near the sea surface (e.g., Chambers et al., 1997; Boccaletti et al., 2004; Willis et al., 2004; Du et al., 2005). This is due largely to the fact that the oceanic mixed layer gives rise to small scale variability with longer persistence times than the variability associated with such scales in the atmospheric boundary layer (e.g., Stull, 1988). Atmospheric variables at/near the sea surface (e.g., net solar radiation wind speed, etc.) play substantial roles in driving the seasonal variations in SST.

The major focus of this study is to quantify the relationship between atmospheric variables and SST, given the fact that mechanisms by which climatological variations in SST are tied to atmospheric forcing are poorly understood. For example, a few

modeling investigations (Palmer and Sun, 1985; Barnston, 1994; Kushnir and Held, 1996) and observational studies (Cayan, 1992) examined the the influence of atmospheric variables on SST, but did not investigate the relationship between the two over the global ocean. Some other studies applied the heat flux as a forcing function (e.g., Eden and Willebrand, 2001; Gulev et al., 2003, 2007) in investigating the role of SST in ocean climate simulations but did not specifically explore impact of individual atmospheric forcing variables on seasonal variability of SST. Kara et al. (2009a) explored effects of various near-surface atmospheric variables in controlling the seasonal cycle of climatological SST over the global ocean, but they did not provide any quantitative results.

The relationship between atmospheric variables and SST is of importance to both observational researchers and climate modelers (e.g., ocean and coupled atmosphere-ocean modelers) for various applications. In particular, an ocean modeler would be interested in knowing which atmospheric variable may result in the largest deficiencies in model-simulated SST, and should therefore pay specific attention to its accuracy before using it for a model simulation. This is due to the fact that atmospheric forcing products have their unique biases over the global ocean (Rienecker et al., 1996; Trenberth and Caron, 2001).

* Corresponding author.
E-mail addresses: birol.kara@nrlssc.navy.mil (A.B. Kara), alan.wallcraft@nrlssc.navy.mil (A.J. Wallcraft), harley.hurlburt@nrlssc.navy.mil (H.E. Hurlburt), loh@stat.wisc.edu (W.-Y. Loh).
[1] www.7320.nrlssc.navy.mil

In this paper, the relationship between a given atmospheric variable and SST is addressed by answering the question, "how much variation in a given atmospheric variable (e.g., net shortwave radiation) results in a quantitative change in SST (e.g., 1 °C). Regions where large/small SST changes resulted from a particular atmospheric variable are mapped over the global ocean. This is done using an OGCM. Our hypothesis is that variations in climatological monthly mean SSTs are largely determined by atmospheric variables in ocean model simulations that are performed with no assimilation of or relaxation to any SST data.

Accordingly, the paper is organized as follows. A brief description of the OGCM and simulations from the model are given in Section 2. The procedure for analyzing the relationship between atmospheric variables and SST is introduced in Section 3. Results are demonstrated at selected individual locations in Section 4 and over the global ocean in Section 5. A fractional factorial design study for the model SST errors is presented in Section 6. Conclusions of the paper are given in Section 7.

2. Ocean model

2.1. HYCOM description

The HYbrid Coordinate Ocean Model (HYCOM) includes a large suite of physical processes and incorporates numerical techniques that are optimal for dynamically different regions of the ocean. It contains five prognostic equations: two for the horizontal velocity components, a mass continuity or layer thickness tendency equation and two conservation equations for a pair of thermodynamic variables, such as salt and potential temperature or salt and potential density (Bleck, 2002).

The model behaves like a conventional σ (terrain-following) coordinate model in very shallow oceanic regions, like a z-level (fixed-depth) coordinate model in the mixed layer or other unstratified regions, and like an isopycnic-coordinate model in stratified regions. The optimal coordinate is chosen every time step using a hybrid coordinate generator. The ability to adjust the vertical spacing of the coordinate surfaces in HYCOM simplifies the numerical implementation of several physical processes, such as mixed layer detrainment, convective adjustment, etc, making it a candidate to investigate SST variations over the global ocean.

The HYCOM domain used in this paper spans the global ocean from 78°S to 90°N. It has a 0.72° equatorial Mercator grid between 78°S and 47°N, with an Arctic bi-polar grid north of 47°N, but with latitudinal resolution doubled near the equator. The model has $0.72° \times 0.72° \cos(\text{lat})$ (longitude × latitude) resolution on a Mercator grid. There are 26 hybrid layers in the vertical. The atmospheric forcing is discussed in Section 2.2. Monthly mean temperature and salinity from the Generalized Digital Environmental Model, version 3 (GDEM3) climatology (Carnes, 2009) are used to initialize the model. The simulations use realistic bottom topography with the model boundary at the 50 m isobath. The K-Profile Parameterization (KPP) mixed layer submodel of Large et al. (1997) is used in the simulations.

The model includes computationally efficient bulk heat flux parameterizations for latent and sensible heat fluxes which include stability-dependent exchange coefficients (Kara et al., 2005a). Because there is no relaxation to any SST climatology, most effects of atmospheric variables are taken into account through net surface energy balance in the model (Kara et al., 2005b). This further confirms the appropriate use of an atmospherically-forced model (i.e., with no oceanic data assimilation) in exploring the relationship between atmospheric variables and SST. Note that the SST seasonal cycle is also influenced by various dynamical processes, such as atmospheric advection and oceanic upwelling (Sutton and Allen,

1997; Scott, 2003; Wang and Chang, 2004). However, our hypothesis is that these processes are also related to the atmospheric atmospheric variables, i.e., the ocean model (i.e., HYCOM) takes these effects into account in the upper ocean with the mixed layer submodel, finally resulting in a SST.

2.2. Atmospheric forcing and model simulations

The model was first run for 5 years until statistical equilibrium was reached and then extended for another four years. Our experience is that four model years is enough to equilibrate SST, primarily because this is a direct response to the atmospheric forcing. For example, there is almost no difference between the monthly mean SST from year 5 and year 9 of the standard forcing case. As an example, we ran the model for about 25 years, demonstrating almost no changes in the mean of basin-averaged net heat fluxes and SST over the global ocean (Fig. 1).

Climatological monthly means of atmospheric forcing variables were formed from the $1.125° \times 1.125°$ European Centre for Medium-Range Weather Forecasts (ECMWF) 40-year re-analysis over the years 1979–2002 (Uppala et al., 2005). For example, the January mean is the average of all Januaries from ERA-40 from 1979 to 2002. A climatological mean correction is applied to some fields obtained from ERA-40 to improve their accuracy. Winds are improved by using the satellite winds (QuikSCAT) as described in Kara et al. (2009b). Zonal and meridional components of wind stress are then computed following Kara et al. (2007). A high frequency component is added to the climatological winds, i.e., the wind forcing includes 6-h variability added to the monthly means (e.g., Kara et al., 2005c). This variability is added because the mixed layer is sensitive to sub-monthly changes in surface forcing down to time scales of a day or less. A correction for shortwave and long-
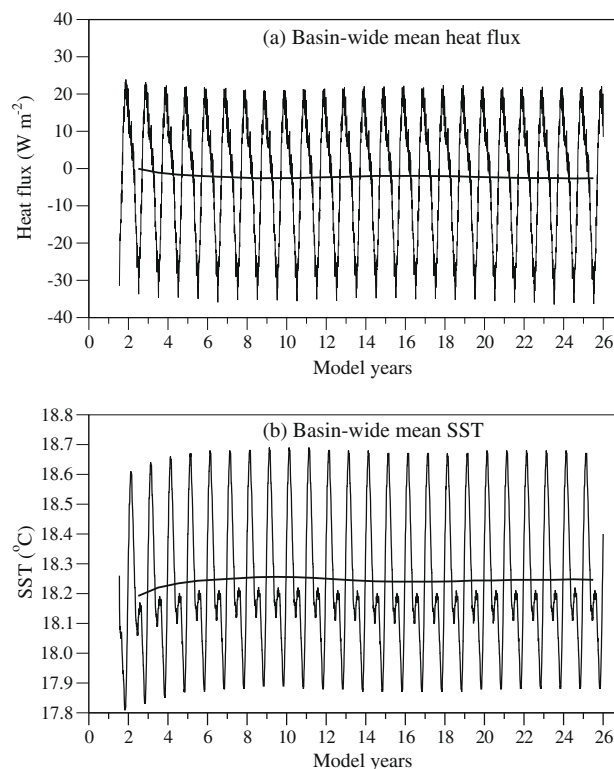

Fig. 1. Basin-wide variations of (a) mean heat flux and (b) mean SST as obtained from the 0.72° global HYCOM for the seasonal cycle and long-term mean.

Table 1
Descriptions of atmospheric forcing variables used for HYCOM simulations. Annual mean represents the average of climatological monthly mean values from ERA-40.

Simulation	Atmospheric forcing used for the ocean model simulation
Monthly	Monthly mean atmospheric forcing for each variable
Airtemp	The same as simulation 1 but annual mean airtemp
Precip	The same as simulation 1 but annual mean precip
Vapormix	The same as simulation 1 but annual mean vapormix
Shortwave	The same as simulation 1 but annual mean shortwave
Longwave	The same as simulation 1 but annual mean longwave
Windspd	The same as simulation 1 but annual mean windspd
Annual	Annual mean atmospheric forcing for each variable

Fig. 2. Climatological annual (long-term) mean SSTs as obtained from the NOAA OI climatology during 1971–2000. The numbers (1–6) on the map mark the six locations that will be used in the analysis in Section 4.

wave fluxes from ERA-40 is made using data from the International Satellite Cloud Climatology Project (ISCCP) (Rossow and Zhang, 1995). Precipitation at the sea surface is corrected using data from the Global Precipitation Climatology Project (GPCP) (Adler et al., 2003).

Description and units of these atmospheric forcing variables are as follows: air temperature (airtemp) at 10 m above the surface (°C); precipitation (precip) (m s^{-1}); mixing ratio (vapmix) of air at 10 m above the surface (g kg^{-1}); net shortwave radiation (shortwave) at the surface (W m^{-2}); net longwave radiation (longwave) at the surface (W m^{-2}); wind speed (windspd) at 10 m above the surface (m s^{-1}); and wind stress (N m^{-2}).

We would like to investigate changes in the model SST resulting from changes in atmospheric variables, and quantify these changes for each variable, separately. Thus, eight simulations which are twins of the standard simulation are used (Table 1). The standard HYCOM simulation was performed using the monthly means of six atmospheric variables. Each of the other simulations is identical to the standard one except that the climatological annual mean of a chosen atmospheric variable (calculated from the 12-monthly means at each model grid) is used. For example, as shown in Table 1, one simulation was performed with climatological annual mean of air temperature and with monthly means for all other atmospheric parameters given in the table. This simulation is denoted as "airtemp" to indicate that it is the twin of the standard monthly simulation but uses "annual mean air temperature". The same explanation applies to the other simulations. In all simulations, wind stress forcing in the momentum equation is left alone precisely because it dominates ocean dynamics, such as ocean currents. When we use annual mean wind speed, there is some inconsistency in separating wind speed and wind stress, but the same is true to some extent when we hold any single atmospheric field at its annual mean.

None of the simulations discussed in this paper include oceanic data assimilation except for weak relaxation to monthly sea surface salinity from Polar Science Center (PSC) Hydrographic Climatology (PHC) (Steele et al., 2001). This relaxation is designed to keep the evaporation-precipitation balance on track in the model. All model results presented in the following sections are based on monthly means that were constructed from the last year of the simulations.

3. Data and methodology

3.1. Monthly SST bias from the model simulations

We first examine the accuracy of SSTs obtained from each HY-COM simulation given in Table 1. For validations, monthly mean SSTs from HYCOM are formed from daily model outputs, and compared to those from National Oceanic and Atmospheric Administration (NOAA) optimal interpolation (OI) climatology (Reynolds
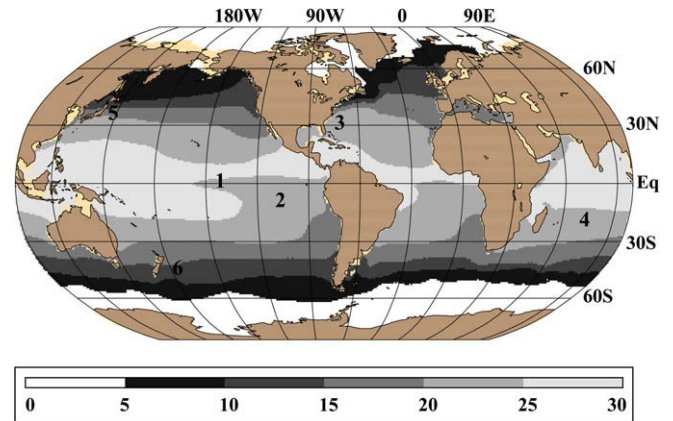
et al., 2002). The NOAA climatology is based on in situ and satellite SSTs. Climatological mean SST from this product is shown in Fig. 2. The NOAA climatology is specifically chosen for model evaluations because its resolution (1° × 1°) is close to that of HYCOM. The NOAA SSTs are interpolated to the model grid for model-data comparisons.

Monthly mean bias is computed by subtracting NOAA SSTs from HYCOM SSTs at each grid point over the global ocean. The resulting SST biases (i.e., HYCOM–NOAA) are shown for months of February, August and November (Fig. 3a–c). These months are just chosen for illustrative purposes. Note that in all maps, regions where ice exists (shown in gray) are excluded from the analysis, because our major focus is SST rather than ice. The ice-free regions are determined from an ice-land mask from the NOAA ice climatology. The mask is a function of the ice analysis and changes by month. For simplicity, in all panels we use the same climatological mask, which is the mask of maximum ice extent.

The standard HYCOM simulation, which is forced with monthly means of atmospheric variables, gives the smallest SST bias, including for all individual months (Fig. 3). Relatively large SST biases exist in the regions where western boundary currents are located because the resolution of the model used in this paper is not sufficient to resolve these current systems. Otherwise, HYCOM SST errors are within ±0.5 °C over the majority of the global ocean. When the model is forced with the annual mean of any particular atmospheric variable and monthly means for others, SST bias typically increases. For example, there are large biases for the simulations of vapormix, shortwave and longwave. Such biases, in part, reveal the impact of that particular atmospheric variable in simulating the seasonal cycle of SST. There are clearly spatial variations in SST errors. When comparing results for the month of August from the standard monthly simulation with the simulation that uses the annual mean of shortwave radiation, the latter simulates model SST that is too cold (by >2 °C) at high northern latitudes, including both the Pacific and Atlantic Oceans. For this reason, shortwave radiation can play a significant role in driving the seasonal cycle of SST in those particular regions.

In the bottom panels of Fig. 3, the model SST errors compared to the NOAA climatology are from the simulation forced with annual means of all atmospheric variables. This is the worst case, as one would expect. SST biases are consistent; in other words, there are warm (cold) biases in the northern hemisphere winter (summer) and vice versa in February and August. The simulation forced with the annual mean of all atmospheric variables yields nearly constant SST with almost no seasonal variation at a given location.
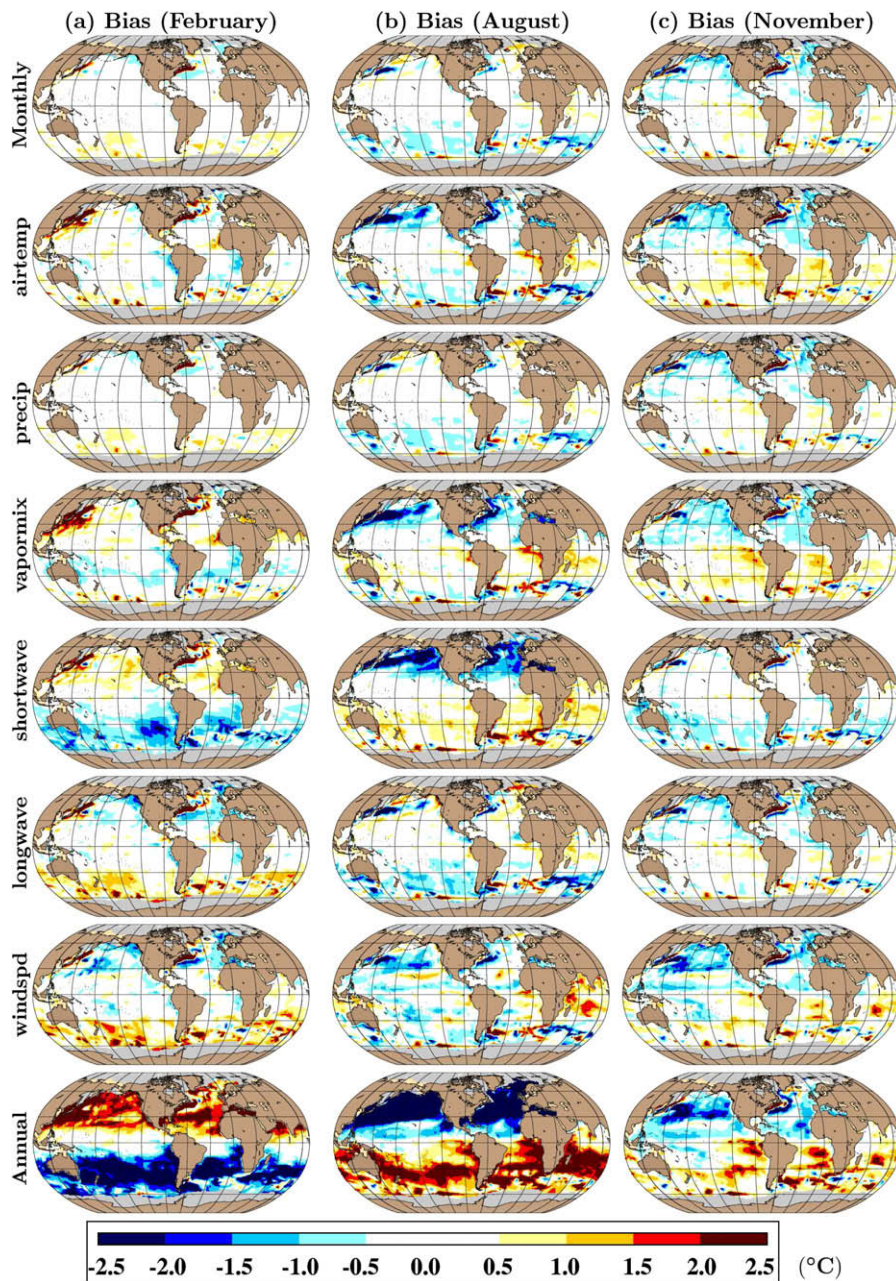
Fig. 3. Monthly mean SST bias (HYCOM–NOAA) for the climatologically-forced model simulations (see Table 1) in comparison to the NOAA SST climatology.

This result is a necessary condition for the approach used in this study. Here, one or more atmospheric variables is held to the annual mean, while the remaining include the climatological seasonal cycle.

3.2. Procedure for the analyses

In addition to the monthly mean SST values, annual and monthly means of atmospheric variables will be used in the analysis. The monthly SST values are constructed from HYCOM simulations forced with either the monthly or annual mean of a given atmospheric variable, a combination that is varied in different model simulations (Table 1). The atmospheric forcing variables are from ERA-40 interpolated to the 0.72° model grid. Based on the analysis procedure below, we first examine the possible relationship between each atmospheric variable and SST (e.g., air tem-

perature versus SST, precipitation versus SST, vapor mixing ratio versus SST, etc.) at a few individual locations (Section 4). The same analysis is then extended to the global ocean (Section 5). The steps for the analysis procedure are as follows:

(1) Monthly mean SSTs from each climatologically-forced HYCOM simulation are obtained at each model grid point over the global ocean. As described in Table 1, these simulations are labeled as monthly, airtemp, precip, vapormix, shortwave, longwave, windspd and annual. The monthly simulation is the standard experiment, as defined in Table 1.

(2) SST differences between a simulation that uses the annual mean of a given atmospheric variable and monthly means otherwise and the standard monthly simulation are then calculated. For example, monthly mean SSTs from the standard simulation are subtracted from those obtained from the

airtemp simulation for each month over the seasonal cycle (i.e., from January to December). This process yields 12 monthly mean SST difference values at each grid point. The same procedure is repeated for other simulations.

(3) The monthly mean of each atmospheric variable used for the standard model simulation is extracted at each model grid point over the global ocean over the seasonal cycle.

(4) Similarly, the annual mean of each atmospheric variable is obtained based on the monthly mean values at each model grid point.

(5) Differences between annual and monthly values of each atmospheric variable are formed. For example, the climatological annual mean of air temperature is subtracted from the monthly mean of air temperature. This means that the same annual mean air temperature value at a given model grid point is subtracted from the monthly means from January to December, yielding 12 mean atmospheric forcing difference values at each model grid. The same procedure is repeated for other atmospheric variables.

A notable point here is that the climatological mean SSTs from the standard monthly HYCOM simulation are being treated as representative of the truth. This is confirmed by the analysis presented in Section 3.1 which discusses the accuracy of HYCOM SSTs in comparison to NOAA climatology (see Fig. 3). Using the same standard atmospheric forcing in HYCOM simulations and switching to the annual mean of a single atmospheric variable at a time allows us to explore the relationship between the single atmospheric variable versus SST in a consistent way.

3.3. Linear regression

In Sections 4 and 5, linear regression will be used to examine the relationship difference between atmospheric variables differences (annual-monthly) and SSTs differences obtained from two HYCOM simulations: one forced with the annual mean of a given variable with monthly means for other variables and the other with monthly means of all variables (Table 1). We provide only a brief description of linear regression analysis as used in this study. A more extensive summary can be found in Neter et al. (1988) and Wilks (1995).

We will evaluate time series of differences in atmospheric variables and SST over the seasonal cycle at every ice-free point on the global model grid. The statistical relationships between monthly mean differences in atmospheric variables (X) and those in SST (Y) are expressed as follows:

$$R = \frac{1}{n-1} \sum_{i=1}^{n} (X_i - \overline{X})(Y_i - \overline{Y})/(\sigma_X \sigma_Y), \tag{1}$$

$$Y = a + bX + c \tag{2}$$

where $n = 12$, R is the correlation coefficient and $\overline{X}(\overline{Y})$ and $\sigma_X(\sigma_Y)$ are the means and standard deviations of atmospheric variables (SST) values, respectively. In the regression Eq. (2), Y is the
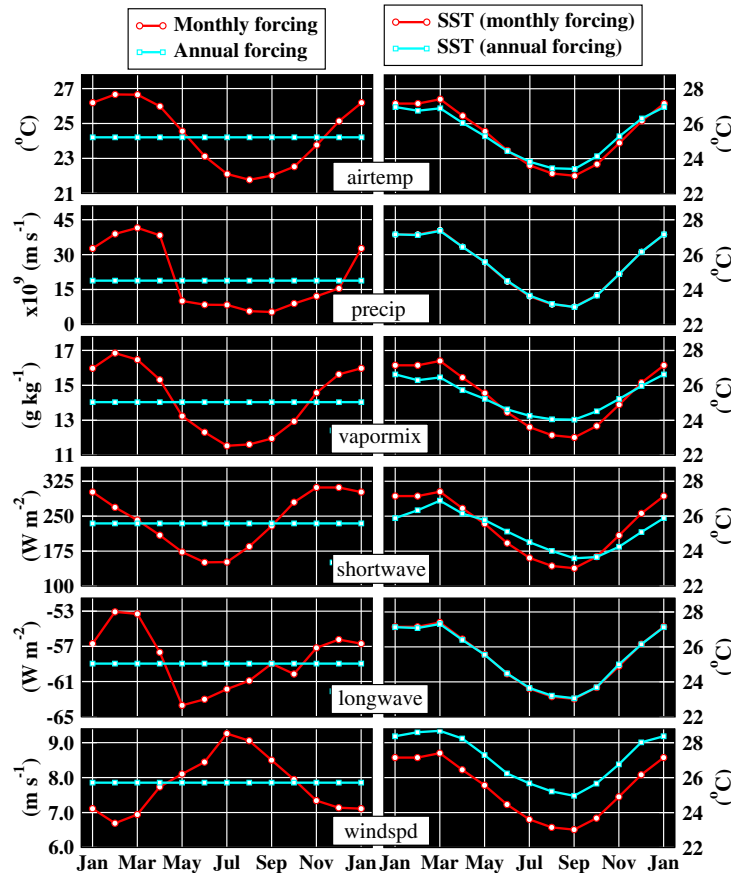

Fig. 4. Climatological monthly and annual means of atmospheric variables (left column) at (20°S, 070°E), location 4 marked on Fig. 2. Also included are monthly mean SST time series (right column) when HYCOM is forced with the monthly mean of each atmospheric forcing variable (monthly) and using twins of this simulation, i.e., all monthly forcing except for the annual mean of one variable at a time. For example, airtemp stands for the model simulation that is forced with annual mean air temperature but monthly means for other atmospheric forcing variables (i.e., precip, vapormix, shortwave, longwave and windspd).
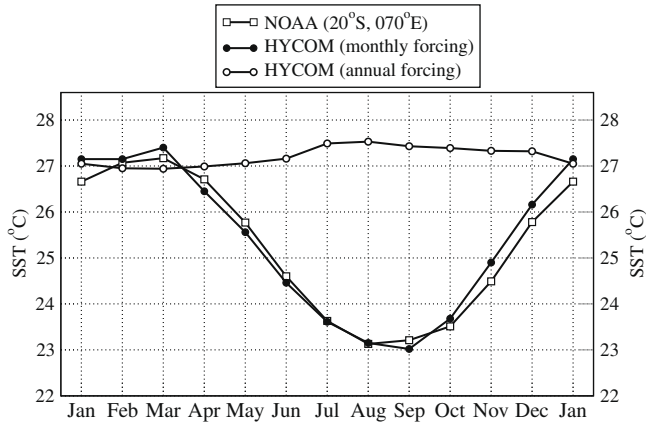
Fig. 5. Comparisons of climatological monthly mean SST time series at (20°S, 070°E). Comparisons are made between NOAA SST climatology and those obtained from two climatologically-forced HYCOM simulations: one (i.e., monthly) uses the monthly mean of each atmospheric forcing variable, and the other (annual) uses annual means of all atmospheric forcing variables.

dependent variable, X is the independent variable (or covariate), a is the intercept, b is the slope or regression coefficient and c is the

error term. The regression equation will specify the average magnitude of the expected change in SST for the given variation in atmospheric variable. The strength of the linear relationship between differences in SST and atmospheric variables is determined by the R value (see (1)), which ranges from −1 to 1. An R value of −1 (1) indicates a very strong negative (positive) linear relationship, and an R value of 0 indicates no linear relationship.

In the analyses, we do not remove the seasonal cycle from the time series. Taking out the seasonal effects from each variable and then testing the correlation of the residuals answers a different question, which is not the focus of this paper. In other words, we are not investigating whether the two variables (SST and a given atmospheric variable), are uncorrelated after the seasonal effects are removed. The question we would like to answer is "how much change in SST, on average, results from a unit change in a given atmospheric variable?" The problem lies with the statistical significance of the estimated slopes, which we obtain by testing the significance of the correlations.

4. Relationship between atmospheric variables and SST

To demonstrate the analysis procedure, we apply steps (1) through (5) discussed in Section 3.1 and the statistical analysis
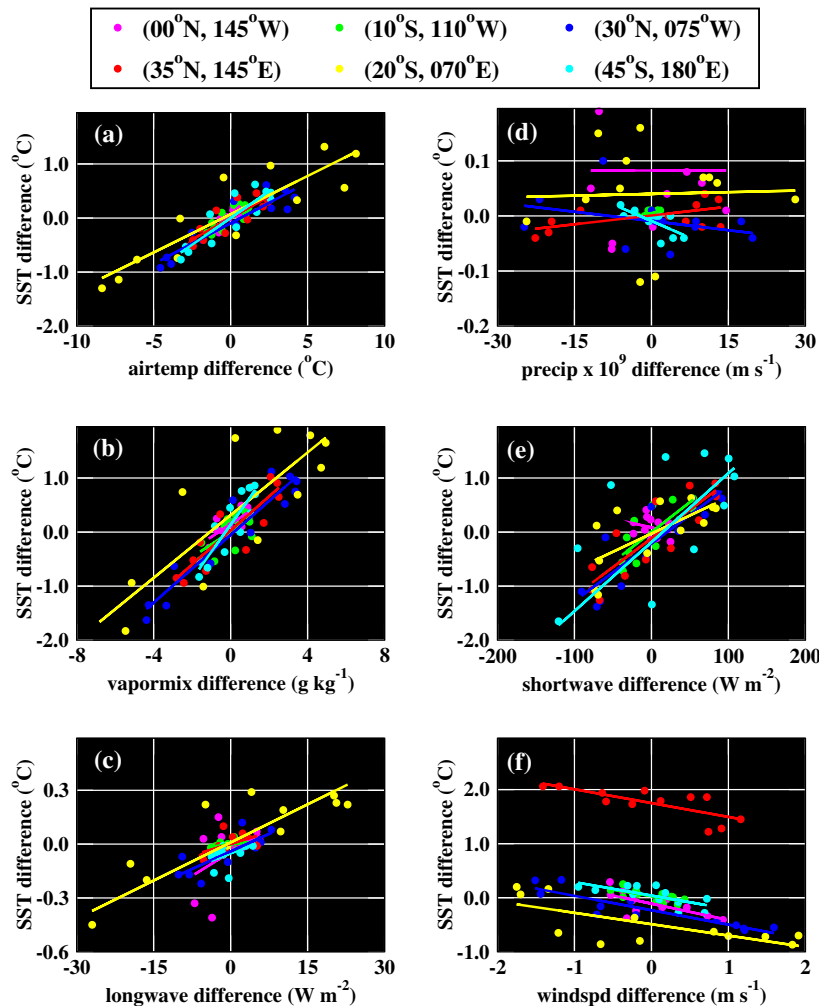

Fig. 6. Scatter plots between differences in SST and those in atmospheric forcing variable at six locations shown in Fig. 2. The SST difference is obtained between the standard simulation forced with monthly mean atmospheric forcing variables and the simulation forced with annual mean of a given atmospheric variable (e.g., airtemp, precip, etc.) with monthly means for other variables. Similarly, the differences in atmospheric forcing are obtained by subtracting the annual mean of a given atmospheric variable from the monthly means.

presented in Section 3.2 at selected locations. Atmospheric variables (climatological monthly and annual means) and monthly mean SSTs obtained from the different HYCOM simulations are obtained at six locations. These point locations are chosen to represent various geographical regions of the global ocean (Fig. 2). The same analysis procedure will then be used in Section 5 to obtain more general results over the global ocean.

There are strong seasonal variations in atmospheric variables evident at (20°S, 070°E) as seen from (Fig. 4). This point is marked as location 4 in the southern Indian Ocean (Fig. 2). The largest changes in SST are noted when the model is forced with annual mean wind speed and monthly means of other atmospheric variables. Not surprisingly, the Indian Ocean generally experiences the northeast and southwest monsoons. The northeast monsoon (e.g., winter) is characterized by steady but moderate winds, while the southwest monsoon (summer) is characterized by strong winds. Shallow and deep ocean mixed layer formation typically results from such changes in wind speed in the upper ocean in this region (Kara et al., 2003). Relatively high wind speeds depress SST year around compared to the weak annual mean which occurs because the relatively strong winds reverse direction over the seasonal cycle. Thus, wind speed at this specific location is the most important atmospheric variable in driving the SST variations.

Because there is strong seasonal variability in the atmospheric forcing, HYCOM forced with the annual mean of all atmospheric variables (airtemp, precip, vapormix, shortwave, longwave and wind speed) gives very unrealistic SSTs in comparison to the standard simulation using the monthly mean of all atmospheric forcing variables (Fig. 5). The SST from the standard HYCOM simulation agrees remarkably well when compared to the satellite-based NOAA SST climatology. At this location, the RMS SST difference for the standard all monthly (all annual) simulation with respect to the NOAA SST climatology is 0.26 °C (2.70 °C) over the seasonal cycle.

There are also large changes in SST when the model is forced with the annual mean of vapormix, shortwave and wind speed as opposed to the standard monthly simulation. For instance, in the case of the model simulation using annual mean wind speed, there is a systematic warm SST bias (≈2 °C) in comparison to the standard monthly simulation. Net shortwave radiation at the sea surface has a large seasonal cycle. The difference in monthly and annual shortwave radiation values is 80 W m^{-2} (−80 W m^{-2}) in January (July), and the HYCOM simulation using the annual mean shortwave radiation gives a warm (cold) SST bias of 1 °C when forced with annual mean shortwave radiation and monthly means for other variables.

When there is almost no difference between annual and monthly mean shortwave radiation values in March and September, HYCOM gives the same SST value, as expected. The main point here is that while both shortwave radiation and wind speed have large seasonal variations, the simulated SST from the model using annual mean shortwave radiation and wind speed with monthly means for other variables are not very similar. This indicates that, for example, a 1 °C warming or cooling in SST in comparison to the standard simulation does not result from the same percentage change in the atmospheric variable. Quantifying such changes in SST with respect to the different atmospheric variables will be our major focus.

Time series of monthly and annual mean atmospheric variables and model-simulated SSTs obtained using those variables presented at (20°S, 070°E) in Fig. 4 demonstrate that there could be a simple linear relationship between atmospheric variables and SSTs. For example, when annual mean air temperature is colder (warmer) than the monthly mean air temperature for a given month, SSTs simulated by HYCOM forced with the annual mean of air temperature and monthly mean for other variables are typically colder (warmer) than those obtained from the standard monthly simulation at both locations. The similar explanation also applies to the mixing ratio and shortwave radiation.

For the reasons mentioned just above, we now investigate whether or not the difference (annual-monthly) in atmospheric variables are linearly correlated to the difference (annual-monthly) in model-simulated SST over the 12-month period. In other words, using the time series (20°S, 070°E) from the left and right columns in Fig. 4, we simply form differences of atmospheric variables and SSTs for each month over the seasonal cycle. This process is repeated at the five other locations from Fig. 2.

Table 2

Statistics between differences in atmospheric variables and SSTs over the seasonal cycle. Linear correlation coefficients, slope and standard error for coefficients obtained from the regression analysis, as described in Section 3.2, are given. Differences in atmospheric variables are calculated using annual and monthly means over the seasonal cycle, and those in SSTs are obtained from the HYCOM simulation forced with the annual mean of a given variable with monthly means for other variables and the standard HYCOM simulation using all monthly mean atmospheric forcing. The reader is referred to Section 3.1 for details of the calculation procedure.

	Airtemp (°C/°C)	Precip (°C/m s^{-1})	Vapormix (°C/g kg^{-1})	Shortwave (°C/W m^{-2})	Longwave (°C/W m^{-2})	Windspd (°C/m s^{-1})
Correlation						
1: (00°N, 145°W)	0.81	0.00	0.73	−0.27	0.48	−0.69
2: (10°S, 110°W)	0.72	0.45	0.65	0.79	0.37	−0.69
3: (30°N, 075°W)	0.92	−0.35	0.95	0.87	0.81	−0.91
4: (20°S, 070°E)	0.85	0.57	0.87	0.85	0.55	−0.75
5: (35°N,145°E)	0.89	0.03	0.84	0.68	0.83	−0.71
6: (45°S, 180°E)	0.88	−0.71	0.89	0.72	0.52	−0.70
Slope						
1: (00°N, 145°W)	0.26	0.00	0.24	−0.003	0.018	−0.30
2: (10°S, 110°W)	0.16	0.00	0.23	0.011	0.003	−0.24
3: (30°N, 075°W)	0.15	0.00	0.31	0.011	0.013	−0.27
4: (20°S, 070°E)	0.16	0.00	0.32	0.011	0.009	−0.26
5: (35°N, 145°E)	0.14	0.00	0.29	0.007	0.014	−0.21
6: (45°S, 180°E)	0.20	0.00	0.50	0.013	0.011	−0.25
Std. error						
1: (00°N, 145°W)	0.06	0.00	0.07	0.004	0.010	0.10
2: (10°S, 110°W)	0.05	0.00	0.09	0.003	0.002	0.08
3: (30°N, 075°W)	0.02	0.00	0.03	0.002	0.003	0.04
4: (20°S, 070°E)	0.03	0.00	0.06	0.002	0.004	0.07
5: (35°N, 145°E)	0.02	0.00	0.06	0.002	0.003	0.07
6: (45°S, 180°E)	0.03	0.00	0.08	0.004	0.006	0.08

Scatter diagrams of SST differences versus atmospheric variable differences are shown in Fig. 6 for each model simulation forced with the annual mean of airtemp, precip, vapormix, shortwave, longwave and windspd with monthly mean variables for others, separately. An elliptical pattern of SST differences in relation to several types of atmospheric differences is evident at some locations. Hysteresis in the SST response to the atmospheric forcing is evidence of some lag in response, which is neglected in this analysis.

For each case in Fig. 6 we would like to find the best straight line through the differences in atmospheric variables and SST. Thus, the least squares fit is also plotted at each location. Except for precip-

itation, there is generally a strong linear relationship between differences in atmospheric variables and SST at all locations. The strong linear relationship is particularly evident from the large correlation values given in Table 2, explaining that most of the variance (e.g., >60%) in SST differences is explained by the differences in atmospheric variables, especially for airtemp, shortwave and windspd.

Because a simple linear relationship holds between atmospheric variables and SST differences, the slope of the least squares line provides useful information about the value of SST difference resulting from differences of the (annual-monthly) atmospheric variables. For example, slope values for SST versus atmospheric
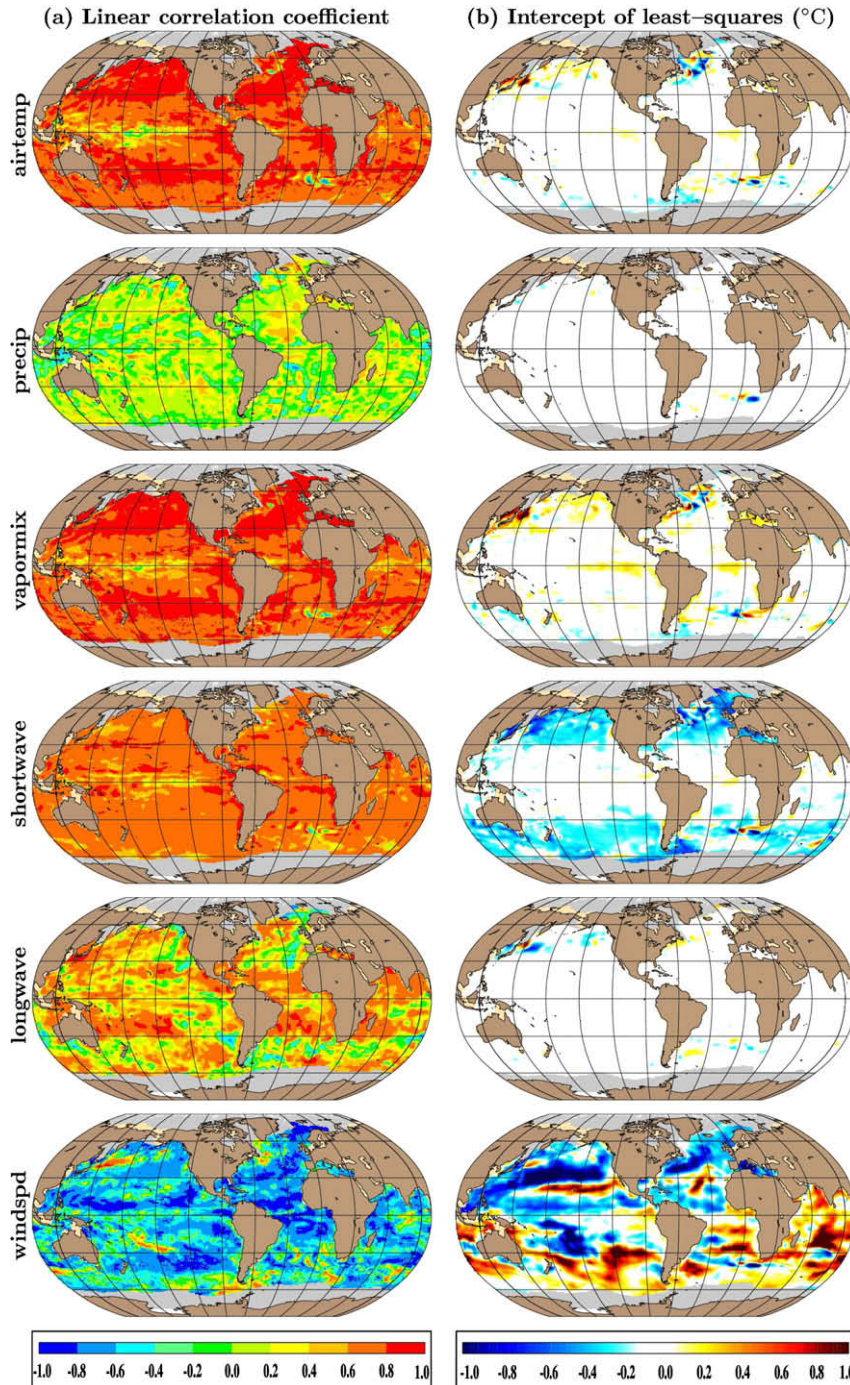

Fig. 7. Spatial variations of (a) correlation coefficient and (b) intercept. Results are provided for each atmospheric forcing variable. Both (a) and (b) are obtained from the least squares approach.

variable differences are 0.011 °C/W m^{-2} and 0.32 °C/g kg^{-1} for simulations using the annual mean shortwave radiation and annual mean vapor mixing ratio with respect to the standard monthly simulation at (20°S, 070°E). These values are based on the least squares fits (Table 2). Based on these slope values, a difference of 100 W m^{-2} (3 g kg^{-1}) between monthly and annual net shortwave radiation (vapor mixing ratio) values results in a SST difference of ≈1 °C. The assumption here is that SST differences from HYCOM are solely controlled by the shortwave radiation and vapor mixing ratio differences for each case.

Unlike other variables, differences in wind speed result in negative but strong correlations with those in SST (Fig. 6 and Table 2). A slope value of −0.26 °C/m s^{-1} at (20°S, 070°E) reveals that an increase of 1 m s^{-1} between monthly and annual mean wind speed gives a decrease of ≈0.26 °C. Standard error for the slope values are usually very small, and can be negligible for most forcing variables.

5. Regression between atmospheric variables and SST

Discussions in the preceding section reveal that there is usually a strong linear relationship between atmospheric forcing variables and SST at six locations. Here, we extend the same analysis to investigate if such relationships also exist over the global ocean. Regression analyses are performed under the assumption that differences in SST are mainly controlled by the differences in a given atmospheric variable. The analysis procedure is already outlined in Section 3.2 (items (1) through (5)). Thus, we use the 12 monthly mean values for air temperature differences and SST differences at each grid point. The dependent (independent) variable is differences in SST (atmospheric variable). Correlation values, intercepts and slopes of the least squares fit are then obtained.

We first find correlation coefficients between the time series of monthly differences for a given atmospheric variable and those for SST when the model is forced with the annual mean of that particular atmospheric variable. This process is repeated at each model grid point for each simulation. We then form a map of correlations over the global ocean (Fig. 7a). Intercept values obtained from the regression analysis are also given (Fig. 7b). In general, there are strong correlations between the differences in atmospheric variables and SST except for precipitation (Fig. 7a). For airtemp there are large positive correlation values but for precip correlations are generally close to zero.

We use a sign test to assess the statistical significance of the distribution of positive and negative values of the correlation coefficients at roughly equally-spaced points over the global ocean.
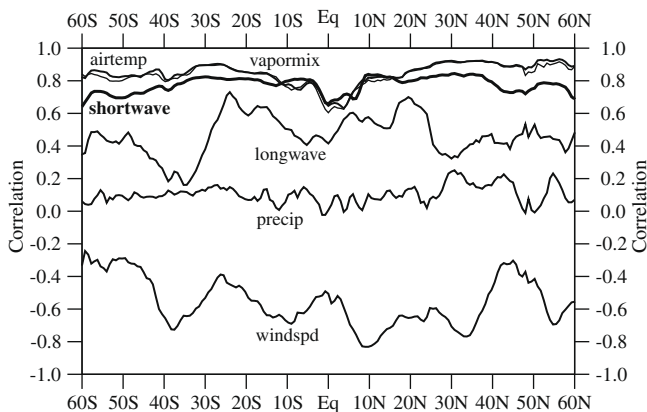
There is a 0.5 probability that the estimated correlation (or slope) at any grid point is positive and a 0.5 probability that it is negative. Let N be the total number of grid points and T the number of positive estimated slopes. For large values of N (as we have here) and at the 0.05 level of significance, the null hypothesis is rejected if $|T − 0.5N| > 0.98\sqrt{N}$. For example, to test whether the correlations for airtemp and precip are significantly different from zero, we apply the sign test to the correlation values in each map. The null hypothesis that there is zero correlation is rejected if the result is significant. Almost 99.3% and 60.8% of the correlation values are positive for airtemp and precip, respectively. Accordingly, correlation values are found to be statistically significant for both airtemp and precip, but the relationship is very weak for the latter as evident from small values.

The largest correlations exist between SST and three atmospheric variables: air temperature, vapor mixing ratio and shortwave radiation. Global averages of correlations are 0.85, 0.86 and 0.78, respectively. For these three variables, correlation values are almost the same at all latitude belts (Fig. 8). Therefore, their impacts in driving the seasonal cycle of SST are generally similar.

When regression analyses are performed between the time series differences of air temperature differences versus SST differences, vapor mixing ratio versus SST and longwave radiation versus SST, intercept values are zero or nearly zero over almost all of the global ocean (Fig. 7b). There is no correlation between monthly mean SST and precipitation differences since they are not statistically different from the zero correlation over most of the global ocean. Therefore, the linear regression analysis for precipitation versus SST is meaningless.

Correlation coefficients between differences in wind speed and those in SST are typically negative with a globally-averaged value
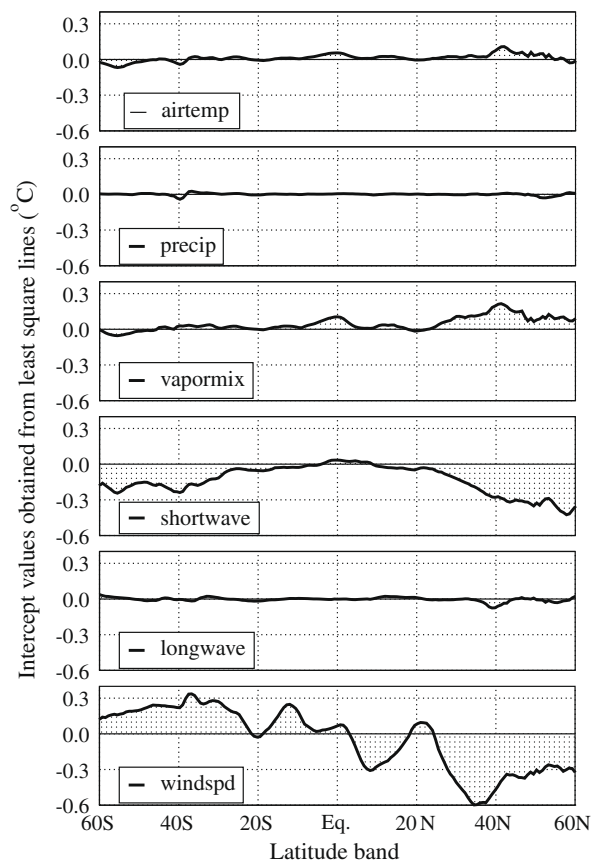
Fig. 8. Zonal averages of correlation values shown in Fig. 7. Note that correlation values for airtemp (thin solid line) and vapormix are very similar. Correlation values for the net shortwave radiation case are shown with a thick solid line.

Fig. 9. Zonal averages of intercept values shown in Fig. 7.

of −0.58. At first, having such a negative relationship between wind speed and SST differences seems to look strange, but note that intercept values are generally large (Fig. 7b), often larger than ±0.5 °C especially at the mid-latitudes. In particular, wind speed is the only variable whose monthly and annual mean differences regressed against differences in SST usually give a non-zero intercept at all latitudes over the global ocean (Fig. 9). It is not surprising that stronger wind speeds produce cooler SSTs since latent heat flux is usually negative and it increases in magnitude with high wind speeds. Also stronger winds would tend to give deeper mixed layer depths and hence again cooler SST.

By far the most important important parameter obtained from linear regression analysis is the slope, which gives change in SST difference per variations in atmospheric variables (Fig. 10). When we assume that differences in model-simulated SST result only from differences in air temperature (i.e., airtemp), given that slope values are 0.15 °C/°C over most of the global ocean, we can indicate that 1 °C in air temperature results in ≈0.15 °C change in SST. However, the same amount of variation in the air temperature gives smaller variations (<≈0.10 °C) in equatorial regions and larger changes (<≈0.20 °C) in SST at mid-latitudes (Fig. 11).

The inverse of slope values is helpful for identifying the change in a given atmospheric variable required to yield a 1 °C warming or cooling in SST (Fig. 12). For example, in general, >100 W m^{-2} difference between annual and monthly mean shortwave radiation is needed to obtain a 1 °C SST change in tropical regions. Here, it must be noted that because correlation (intercept) values are very high (near zero) over most of the global ocean (Fig. 7a and b), the slope values give us quite a precise estimation of the SST change resulting from air temperature, vapor mixing ratio, shortwave and longwave radiation (see Table 2).

In the case of vapor mixing ratio, it is evident from Fig. 10 that a 1 g kg^{-1} difference in vapor mixing ratio gives ≈0.4 °C change in SST at mid- to high-latitudes, but the change in SST obtained from the same vapor mixing ratio difference of ≈1 g kg^{-1} is halved, generally ≈<0.2°, in tropical regions, especially the western equatorial Pacific warm pool. The slope values for shortwave radiation are generally between 0.12 and 0.18 °C/W m^{-2} in mid- to high-latitudes where the intercept of the least squares line is also relatively large in comparison to the other latitudes (Fig. 9). However, there are relatively smaller slope values in the equatorial Pacific, Atlantic (<0.004 °C/W m^{-2}) and most of the Indian Ocean (<0.010 °C/W m^{-2}), where the intercept values are generally close to zero. In the equatorial Pacific, a 1 W m^{-2} (100 W m^{-2}) difference in net shortwave radiation yields only ≈0.004 °C (≈0.4 °C) difference in SST, in comparison to ≈0.015 °C (≈1.5 °C) change at mid- to high-latitudes. The global average of the slope is <0.013 °C/W m^{-2}.

As demonstrated in Fig. 9 earlier, intercept values between differences in longwave radiation and SST are approximately zero at all latitudes. Not surprisingly, slope values are thus almost uniform, having a globally averaged value of <0.007 °C/W m^{-2}, which is about half that of the shortwave radiation (Fig. 10). This confirms that net shortwave radiation at the sea surface has much more influence on the SST seasonal cycle than net longwave radiation at the sea surface. This is especially true in open ocean regions. One should also notice that the relationship between differences in longwave radiation and SST is not as strong as the one between differences in shortwave radiation and SST, as confirmed by correlation values (Figs. 7a and 8). Thus, we do not have the same confidence in the linear relationship between longwave radiation and SST as one has between shortwave radiation and SST.
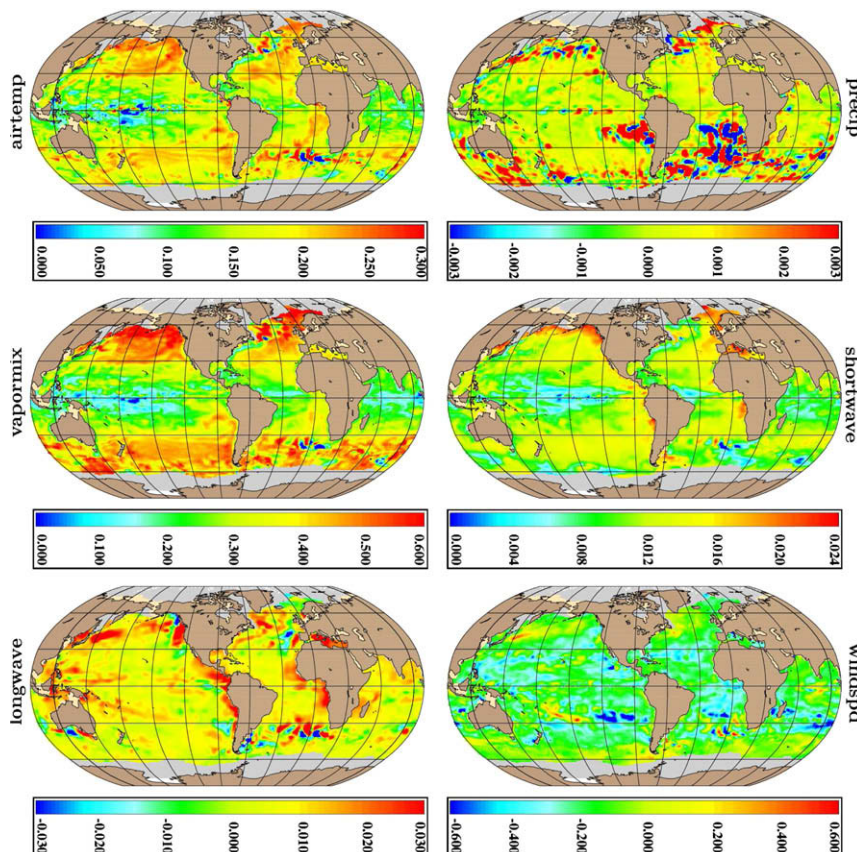

Fig. 10. Spatial variations of slope values obtained from the least squares analysis (see Fig. 7). Note that color bars have different scales for each panel. Units for slope values are as follows: airtemp (°C/°C), precip ($10^{-9} \times$ °C/m s^{-1}), vapormix (°C/g kg^{-1}), shortwave (°C/W m^{-2}), longwave (°C/W m^{-2}) and windspd (°C/m s^{-1}).

In the relationship between wind speed and SST differences, slope values are usually negative (Fig. 10), consistent with negative correlations (Fig. 7a). If there had been a perfect linear relationship with negative slope between the two, we would have had a correlation coefficient of −1. Very high correlations (≈−0.8) exist only in some regions just north of equator. However, they are not statistically significant in comparison to a correlation value of −0.7. On the other hand, since the correlation values are larger than 0.53, they are statistically different from a zero correlation. In this situation, the slope value is ≈−0.2 °C/m s^{-1} between 40°S and 40°N (Fig. 11), i.e., 1 m s^{-1} increase (decrease) in near-surface wind speed results in ≈0.2 °C cooling (warming) in SST, in general.

Wind speed is the only variable whose slope is almost constant in comparison to the other variables (airtemp, vapormix, shortwave and longwave) over the most of the global ocean. However, one is cautioned that the intercept is indeed large over most of the global ocean (Fig. 7b). For instance, the slope (intercept) value is ≈−0.1 °C/m s^{-1} (≈−0.5 °C) in the latitude belt near 40°N. The intercept is certainly dominant, making the slope a little useless. In this case, a 10 m s^{-1} difference in climatological mean monthly and annual mean wind speed, which is quite unusual over the global ocean, gives a 1 °C change in SST simulated by the ocean model forced with monthly means for all variables versus the annual mean of wind speed and monthly means for other variables. Since the intercept (i.e., ≈−0.5 °C) is large, the slope does not describe the actual change in SST properly as expected from correlation values, which are relatively smaller than those for airtemp, vapormix and shortwave.

Slope values given in Fig. 10 are unique for each atmospheric variable as seen from their units. For example, in the 40° latitude belt, a 1 °C warming in SST results from ≈5 °C change in near-surface air temperature, ≈75 W m^{-2} change in net shortwave radia-

tion at the sea surface, and ≈200 W m^{-2} change in net longwave radiation at the sea surface between annual and monthly mean values (Fig. 12). However, what is not clear from these values is whether or not the ≈5 °C-change in near-surface air temperature is as large (or important) as the ≈75 W m^{-2}-change in net shortwave radiation at the sea surface, both of which give the same 1 °C-change in SST. Thus, if one were to examine the impact on SST differences due to per unit differences in atmospheric variables in a fair way, one possibility would be to normalize slope values.

We normalize slope values with the RMS difference calculated between annual and monthly mean of each atmospheric variable over the seasonal cycle, separately. RMS difference at a given location is obtained between monthly and annual mean (repeated 12 months) time series (e.g., see left panels in Fig. 4). For each variable, the slope value (Fig. 10) is then multiplied by the RMS difference at each model grid point. Finally, the SST difference by each normalized atmospheric variable is obtained (Fig. 13). As an example, for the shortwave radiation at the sea surface, RMS (W m^{-2}) multiplied by slope (°C/W m^{-2}) is in °C. Similarly, for the near-surface vapor mixing ratio, RMS (g kg^{-1}) multiplied by slope (°C/g kg^{-1}) is again in °C.

Relatively large (small) RMS × slope values are generally seen at mid- to high-(tropical) latitudes for each variable, especially for airtemp, vapormix and shortwave (Fig. 13). There are almost no changes in SST (almost zero) resulting from changes in precipitation over the global ocean, confirming that essentially, this variable has no major influence in driving the SST seasonal cycle. While Fig. 12 reveals large SST changes due to longwave radiation, especially at high southern latitudes, the relatively smaller normalized SST difference values reveal the minor impact of this variable in
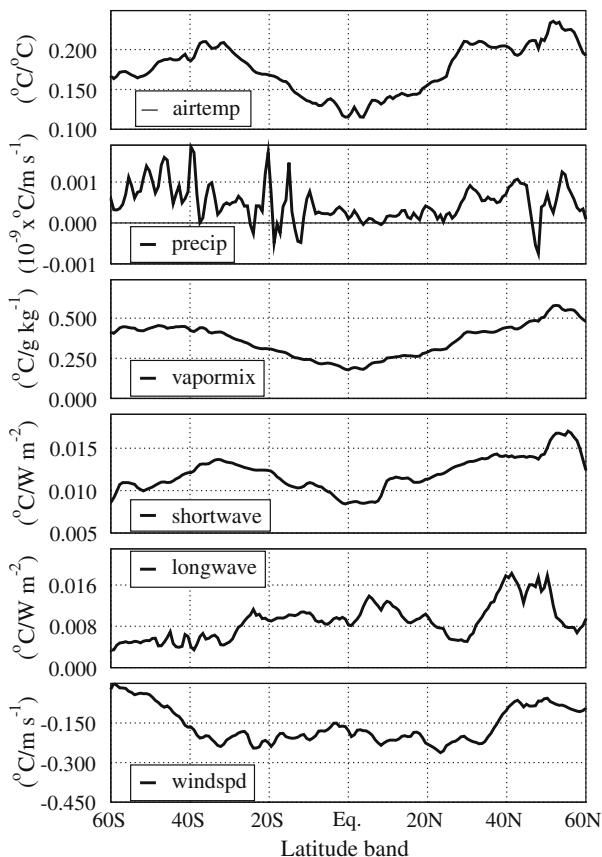

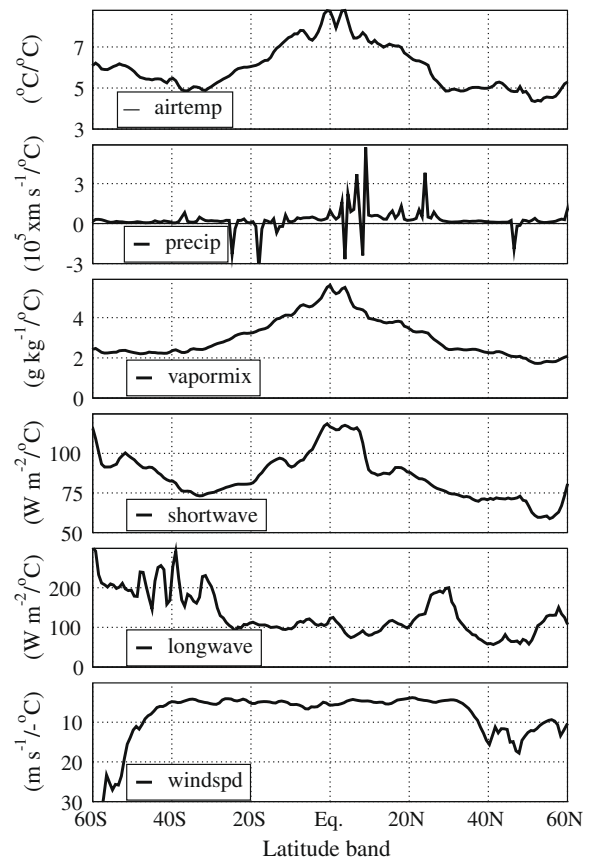**Fig. 11.** Zonal averages of slope values shown in Fig. 10.

Fig. 12. The same as Fig. 11 but the inverse of slope values are given to demonstrate how much change in a given atmospheric variable results in 1 °C warming (or cooling) in SST over the seasonal cycle.
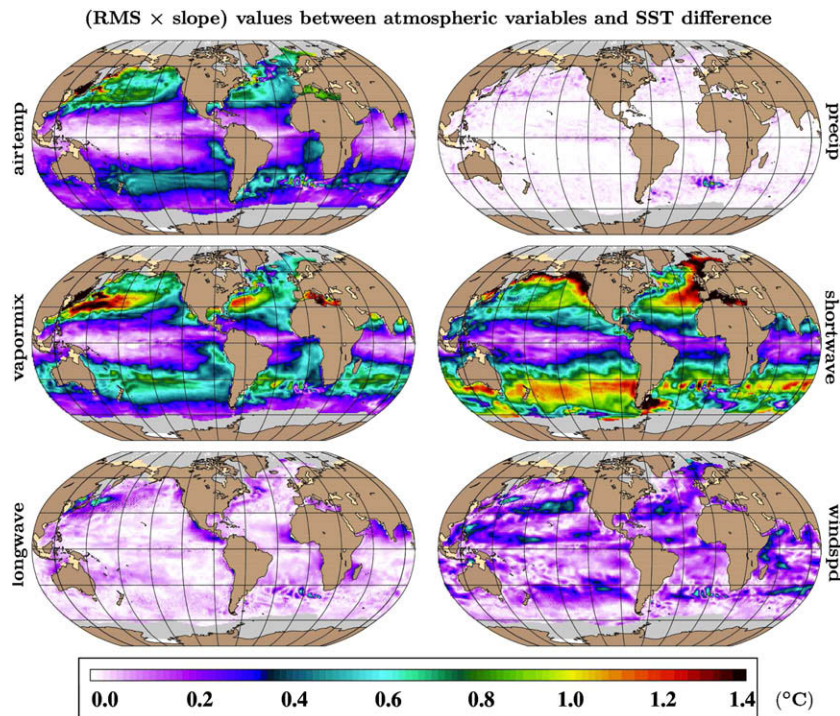
Fig. 13. RMS × slope values over the global ocean. As described in the text, RMS is calculated between monthly and annual means of each atmospheric variable over the seasonal cycle, and slope values are given in Fig. 10. Global averages of RMS × slope values are 0.31, 0.01, 0.45, 0.63, 0.11 and 0.15 °C for airtemp, precip, vapormix, shortwave, longwave and windspd, respectively.

maintaining the SST seasonal cycle. The largest RMS × slope values are evident for the shortwave radiation case over the most of global ocean.

6. Fractional factorial design for SST changes

In Section 5, we examined the change in SST from using monthly versus annual mean of one atmospheric variable at a time. Only one atmospheric variable is changed at a time. We now present the results of a fractional factorial design study, where one or more atmospheric variables are altered simultaneously with the change for each one being a constant increase for all months and all grid points.

The fractional factorial design consists of a total of eight cases as described in Table 3. In each case, the monthly mean of an atmospheric variable is increased at each grid point by a constant amount which is chosen randomly as will be explained below in more detail. The increments are given in the columns of the table, with 0 indicating no increase. For example, in the case of Set 1, the monthly means of atmospheric variables shortwave and longwave are increased by 30 and 60 W m^{-2}, respectively, while the monthly

means of the other four variables are not increased. Such an analysis is known as a two-level fractional factorial design (Box et al., 2005).

Fractional factorial designs are suitable to study the joint effects of many variables using a small number of experiments. There are six atmospheric forcing variables in Table 3. Hence in the present situation, there are $2 \times 2 \times 2 \times 2 \times 2 \times 2 = 64$ ways to increase or not increase the monthly means of the atmospheric variables. A complete examination would require a total of 64 case experiments. Such a study allows estimation of the individual effects of all six variables, as well as all sorts of interactions among them. Following standard statistical terminology, we will call the individual effects as the main effects. As is the case in our situation here, if the increments in the variable values are not large, the interaction effects will typically be dwarfed by the main effects. A fractional factorial design uses this argument to reduce the number of cases to a total of eight. The eight combinations in Table 3 are selected, so that the main effects of the six variables can be estimated. Furthermore, they allow the construction of a model for the combined effects of any or all of the variables.

Various particular values of the increments in Table 3 are chosen, so that the change in SST is physically realistic even when

Table 3
Fractional factorial design for HYCOM simulations. In the table, a "0" indicates that there is no change in the value of the specific variable (i.e., the monthly mean is used). Precipitation values are in units of 1×10^{-8}.

Simulation	Airtemp (°C)	Precip (m s^{-1})	Vapormix (g kg^{-1})	Shortwave (W m^{-2})	Longwave (W m^{-2})	Windspd (m s^{-1})
Set 1	0	0	0	30	60	0
Set 2	2	0	0	0	0	0
Set 3	0	1	0	0	60	2.5
Set 4	2	1	0	30	0	2.5
Set 5	0	0	1	30	0	2.5
Set 6	2	0	1	0	60	2.5
Set 7	0	1	1	0	0	0
Set 8	2	1	1	30	60	0

all the variables are increased simultaneously. If the increase in each variable is expected to yield a 1 °C-increase in SST, then the simultaneous increase in all variables may produce an increase in SST of up to 6 °C, an unrealistically large value. The listed increments for each variable in Table 3 are based on the results in Section 5. Our aim is to allow each variable to produce approximately a 0.4° change in SST. This suggests, for example, a 2 °C increment for airtemp, and a 30 W m^{-2} increment for shortwave. In each column of the table, there are only two different values, with four of each type. For example, under the airtemp column, there are four values of 0 (meaning no increase in airtemp) and four values of 2, which indicates an increase of 2 °C in airtemp.

Unlike the analysis in Section 5, where one atmospheric variable is held constant by replacing the monthly means with an annual mean at each grid point, the cases in Table 3 allow us to construct the following simple statistical model between SST differences and atmospheric variable monthly mean values for each month and grid location:

$$SST_{diff} = b_1 T + b_2 P + b_3 V + b_4 S + b_5 L + b_6 W. \qquad (3)$$

Here $SST_{diff} = SST - SST^*$, where SST is the value when one or more atmospheric variables are increased, and SST* is the value from the standard all monthly simulation (where all variables are unchanged), T = (airtemp increase)/2 °C, P = (precip increase)/10^{-8} m s^{-1}, V = (vapormix increase)/1 g kg^{-1}, S = (shortwave increase)/ 30 W m^{-2}, L = (longwave increase)/60 W m^{-2} and W = (windspd increase)/2.5 m s^{-1}. The values of $b_1, b_2, \ldots, b_6$ are the main effects of the variables at each grid point and each month. They are calculated by fitting a least-squares regression model to the values of the SST differences from the eight simulation experiments. Each b-coefficient thus estimates the change in SST at a particular grid point and month, if the associated atmospheric variable is increased by the amount used in the simulation.

All coefficients of $b_1, b_2, \ldots, b_6$ resulting from Eq. (3) reveal distinct variations over the global ocean (Fig. 14). Results are provided for the three specific months of February, August and November to demonstrate seasonal differences. Other months yield similar values (not shown). For example, a 2 °C increase in airtemp can typically produce a 0.5–0.8 °C increase in SST. Precipitation has almost no influence on SST and typically yields values close to zero. Similarly, a 1 g kg^{-1} increase in vapmix can give up to a >1.0 °C increase in SST.

In the case of wind speed, the resulting b_6 coefficients are negative over most of the global ocean. This is similar to the negative slope values for windspd given in Fig. 10. Note that in the case of the wind speed plot, for consistency we use the same color palette but values must be multiplied by −1. Based on that plot, a decrease of 2.5 m s^{-1} in windspd gives an increase of ≈1.0 °C in tropical regions and at mid-latitudes, and smaller values at other locations.
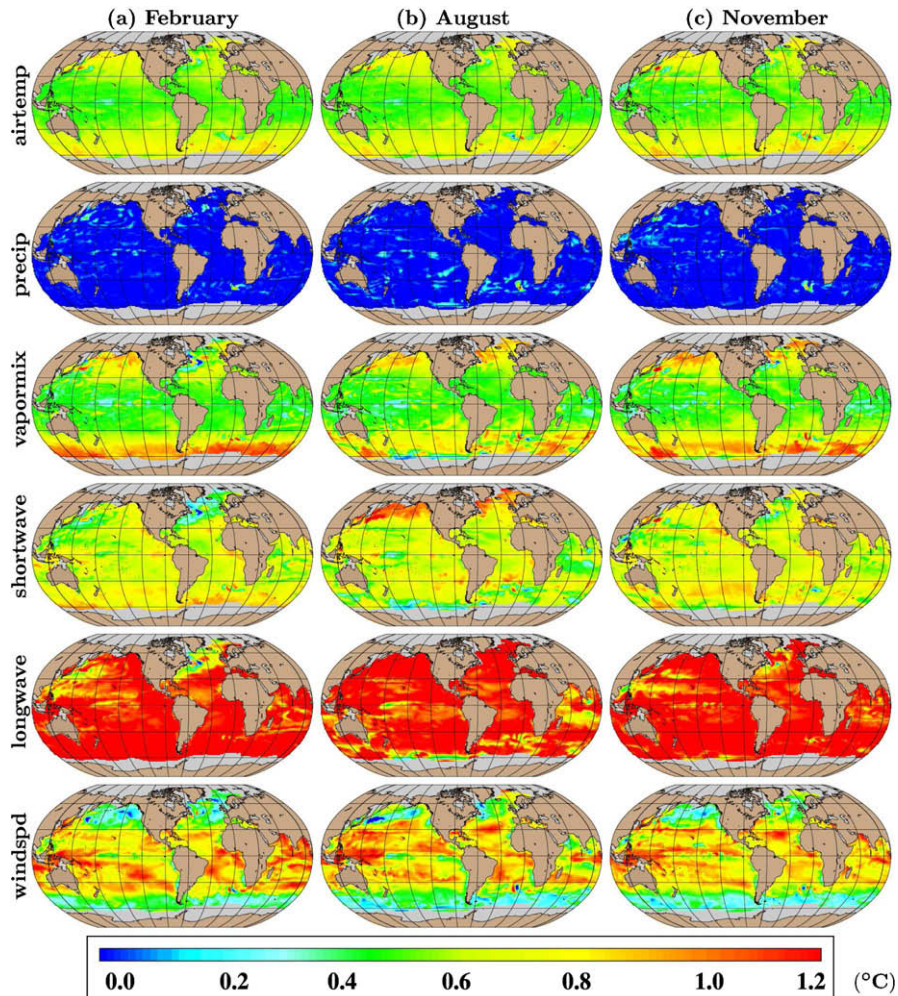

Fig. 14. Spatial variability of increase or decrease in SST based on the b coefficients shown in Eq. (3). The fractional factorial design, which is used for this analysis, is explained in the text, in detail. Note that unlike all the other atmospheric variables, in the case of windspd values in the color palette demonstrate a decrease in SST rather than an increase.

Table 4
Maximum and minimum values of *b*-coefficients from the HYCOM simulations.

	b_1 Airtemp (°C)	b_2 Precip (m s^{-1})	b_3 Vapormix (g kg^{-1})	b_4 Shortwave (W m^{-2})	b_5 Longwave (W m^{-2})	b_6 Windspd (m s^{-1})
Minimum	−0.7978	−1.3248	−1.1616	−0.7292	−1.1483	−1.6362
Maximum	1.8704	1.6747	2.2183	1.8021	3.0453	0.7541

Table 4 gives the minimum and maximum values of the *b*-coefficients over all months and all grid points. They demonstrate, for example, that a 2 °C increase in airtemp can produce up to a 1.87 °C increase in SST and a 0.80 °C decrease in SST. Similarly, a 1×10^{-8} m s^{-1} increase in precip gives up to a 1.67 °C increase in SST and a 1.32 °C decrease in SST.

7. Conclusions

Simulations from a global atmospherically-forced OGCM (HYCOM) with 0.72° resolution and no data assimilation or relaxation to any SST climatology are used to quantify the effects of atmospheric variables at/near the sea surface on monthly mean SST changes over the global ocean. HYCOM includes a realistic mixed layer sub-model, which properly takes physical and dynamical processes in the upper ocean into account, making it a candidate to explore the relationship between SST and atmospheric variables. Model-simulated SSTs from HYCOM with the prescribed atmospheric forcing for the model are analyzed.

Two methodologies were applied to investigate the impacts of various atmospheric forcing variables on SST: (1) linear regression analysis and (2) fractional factorial design. A set of eight simulations was run for the application of each methodology, a different set for each one. The strategy in applying the first methodology was to run (a) one simulation using a monthly mean climatology for every atmospheric forcing variable, (b) six simulations where the annual mean was used for one of the six atmospheric forcing variables and the monthly mean of all the others was used and (c) a simulation where the annual mean of all six thermal forcing variables was used. In all of the simulations a monthly mean wind stress climatology was used as forcing in the momentum equation. Thus, the last simulation included only dynamical effects on the seasonal cycle of SST, such as upwelling and advection, which were generally small in the 0.72° model. The accuracy of SST from each simulation was evaluated in comparison to a satellite-based climatology over the global ocean. To use the regression in testing SST sensitivity to each atmospheric forcing variable individually, the annual mean of each forcing variable, e.g. shortwave radiation, was subtracted from the monthly mean at each model grid point and the monthly mean SST from the simulation in group (b), where that forcing variable was held constant, was subtracted from monthly mean SST in simulation (a). The resulting monthly atmospheric forcing and SST deviation time series were then used in the regression to calculate slope and intercept values at each model grid point over the global ocean.

Linear regression analysis reveals that ≈1° change in SST requires a 6 °C change in air temperature, 3 g kg^{-1} in air vapor mixing ratio, 80 W m^{-2} in shortwave radiation and 150 W m^{-2} in longwave radiation. We find almost no changes in SST due to changes in precipitation over the global ocean, indicating that this particular atmospheric variable does not play any significant role in controlling the seasonal cycle of monthly mean SST. All of these sensitivities vary regionally and relatively low sensitivity is found in tropical regions. In particular, monthly variations in atmospheric variables have significant influences on the climatological mean SST over the seasonal cycle, except in the tropical oceans where dynamical effects can be important (Kara et al., 2009a).

Unlike other atmospheric variables considered in this study, correlations between time series of SST deviations and wind speed deviations over the seasonal cycle are typically weak over most of the global ocean. The linear regression analysis demonstrates that a 1 m s^{-1} increase (decrease) in wind speed gives a negligibly small SST cooling (warming) of ≈0.15 °C. Thus the direct impact of wind speed in driving the SST seasonal cycle cannot be determined because of those low correlations.

While the results from the regression analysis provided useful results, it explored possible relationships between SST and a given atmospheric variable. As a result, it did not include the joint effects of atmospheric variables in controlling the SST seasonal cycle over the global ocean. Therefore, another methodology, a fractional factorial design which allows for nonlinear relationships between SST and atmospheric variables, was also used. In this approach, changes in SST are expressed as functions of changes in all atmospheric variables. The SST error analysis in relation to atmospheric variables based on the fractional factorial design are typically consistent with those based on the simpler least squares approach. This indicates that the model generally responds to changes in atmospheric variables in a linear fashion in predicting SST variability over most of the global ocean.

References

Adler, R.F. et al., 2003. The version-2 Global Precipitation Climatology Project (GPCP) monthly precipitation analysis (1979–present). J. Hydrometeor. 4, 1147–1167.

Barnston, A.G., 1994. Linear statistical short-term climate predictive skill in the northern hemisphere. J. Climate 7, 1513–1564.

Bleck, R., 2002. An oceanic general circulation model framed in hybrid isopyenic-cartesian coordinates. Ocean Modell. 4, 55–88.

Boccaletti, G., Pacanowski, R.S., Philander, S.G.H., Fedorov, A.V., 2004. The thermal structure of the upper ocean. J. Phys. Oceanogr. 34, 888–902.

Box, G.E.P., Hunter, J.S., Hunter, W.G., 2005. Statistics for Experimenters: Design, Innovation, and Discovery, second ed. John Wiley & Sons. 633 pp.

Carnes, M.R., 2009. Description and evaluation of GDEM-V3.0. NRL/MR/7330-09-9165, 21 pp. [Available from Naval Research Laboratory, Stennis Space Center, MS 39529, USA.].

Cayan, D.R., 1992. Latent and sensible heat flux anomalies over the Northern Oceans: driving the sea surface temperature. J. Phys. Oceanogr. 22, 859–881.

Chambers, D.P., Tapley, B.D., Stewart, R.H., 1997. Long-period ocean heat storage rates and basin-scale heat fluxes from TOPEX altimetry. J. Geophys. Res. 102, 10,525–10,533.

Du, Y., Qu, T., Meyers, G., Masumoto, Y., Sasaki, H., 2005. Seasonal heat budget in the mixed layer of the southeastern tropical Indian Ocean in a high-resolution ocean general circulation model. J. Geophys. Res. 110, C04012. doi:10.1029/2004JC002845.

Eden, C., Willebrand, J., 2001. Mechanism of interannual to decadal variability of the North Atlantic circulation. J. Climate 14, 2266–2280.

Gulev, S.K., Barnier, B., Knochel, H., Molines, J.-M., Cottet, M., 2003. Water mass transformation in the North Atlantic and its impact on the meridional circulation: insights from on ocean model forced by NCEP/NCAR reanalysis surface fluxes. J. Climate 16, 3085–3110.

Gulev, S.K., Barnier, B., Molines, J.-M., Penduff, T., Chanut, J., 2007. Impact of spatial resolution of simulated surface water mass transformation in the Atlantic. Ocean Modell. 19, 138–160.

Kara, A.B., Rochford, P.A., Hurlburt, H.E., 2003. Mixed layer depth variability over the global ocean. J. Geophys. Res. 108, 3079. doi:10.1029/2000JC000736.

Kara, A.B., Hurlburt, H.E., Wallcraft, A.J., 2005a. Stability-dependent exchange coefficients for air–sea fluxes. J. Atmos. Oceanic Technol. 22, 1077–1091.

Kara, A.B., Wallcraft, A.J., Hurlburt, H.E., 2005b. A new solar radiation penetration scheme for use in ocean mixed layer studies: An application to the Black Sea using a fine resolution HYbrid Coordinate Ocean Model (HYCOM). J. Phys. Oceanogr. 35, 13–32.

Kara, A.B., Wallcraft, A.J., Hurlburt, H.E., 2005c. How does solar attenuation depth affect the ocean mixed layer? Water turbidity and atmospheric forcing impacts on the simulation of seasonal mixed layer variability in the turbid Black Sea. J. Climate 18, 389–409.

Kara, A.B., Wallcraft, A.J., Metzger, E.J., Hurlburt, H.E., Fairall, C.W., 2007. Wind stress drag coefficient over the global ocean. J. Climate 20, 5856–5864.

Kara, A.B., Wallcraft, A.J., Hurlburt, H.E., Loh, W.-Y., 2009a. Which surface atmospheric variable drives the seasonal cycle of sea surface temperature over the global ocean? J. Geophys. Res. 114, D05101, doi:10.1029/2008JD010420.

Kara, A.B., Wallcraft, A.J., Martin, P.J., Pauley, R.L., 2009b. Optimizing surface winds using QuikSCAT measurements in the Mediterranean Sea during 2000–2006. J. Mar. Syst., doi:10.1016/j.jmarsys.2009.01.020.

Kushnir, Y., Held, I.M., 1996. Equilibrium atmospheric response to North Atlantic SST anomalies. J. Climate 9, 1208–1220.

Large, W.G., Danabasoglu, G., Doney, S.C., McWilliams, J.C., 1997. Sensitivity to surface forcing and boundary layer mixing in a global ocean model: annual-mean climatology. J. Phys. Oceanogr. 27, 2418–2447.

Neter, J., Wasserman, W., Whitmore, G.A., 1988. Applied Statistics, third ed. Allyn and Bacon Press, Massachusetts. 1006 pp.

Palmer, T., Sun, Z., 1985. A modeling and observational study of the relationship between sea surface temperature in the northwest Atlantic and atmospheric general circulation. Quart. J. Roy. Meteor. Soc. 111, 947–975.

Reynolds, R.W., Rayner, N.A., Smith, T.M., Stokes, D.C., 2002. An improved in-situ and satellite SST analysis for climate. J. Climate 15, 1609–1625.

Rienecker, M.M., Atlas, R., Schubert, S.D., Willett, C.S., 1996. A comparison of surface wind products over the North Pacific Ocean. J. Geophys. Res. 101, 1011–1023.

Rossow, W.B., Zhang, Y.-C., 1995. Calculation of surface and top-of-atmosphere radiative fluxes from physical quantities based on ISCCP datasets, Part II: validation and first results. J. Geophys. Res. 100, 1167–1197.

Scott, R.B., 2003. Predictability of SST in an idealized one-dimensional, coupled atmosphere–ocean climate model with stochastic forcing and advection. J. Climate 16, 323–335.

Steele, M., Morley, R., Ermold, W., 2001. PHC: a global ocean hydrography with a high quality Arctic Ocean. J. Climate 14, 2079–2087.

Stull, R.B., 1988. An Introduction to Boundary Layer Meteorology. Kluwer Academic Publishers., Dordrecht. 666 pp.

Sutton, R.T., Allen, M.R., 1997. Decadal predictability of north Atlantic sea surface temperature and climate. Nature 388, 563–567.

Trenberth, K.E., Caron, J.M., 2001. Estimates of meridional atmosphere and ocean heat transports. J. Climate 14, 3433–3443.

Uppala, S. et al., 2005. The ERA-40 re-analysis. Quart. J. Roy. Meteor. Soc. 131, 2961–3012. doi:10.1256/qj.04.176.

Wang, F., Chang, P., 2004. Effect of oceanic advection on the potential predictability of sea surface temperature. J. Climate 17, 3603–3615.

Wilks, D.S., 1995. Statistical Methods in the Atmospheric Sciences. Academic Press, San Diego. 467 pp.

Willis, J.K., Roemmich, D., Cornuelle, B., 2004. Inter-annual variability in upper ocean heat content, temperature, and thermosteric expansion on global scales. J. Geophys. Res. 109. doi:10.1029/2003/JC002260.

Corrigendum

Corrigendum to "Quantifying SST errors from an OGCM in relation to atmospheric forcing variables" [Ocean Model. 29 (2009) 43–57]

A. Birol Kara [a],[*],[1], Alan J. Wallcraft [a], Harely E. Hulburt [a], Wei-Yin Loh [b]

[a] Oceanography Division, Naval Research Laboratory, Stennis Space Center, MS, USA
[b] Department of Statistics, University of Wisconsin, Madison, WI, USA